

Nonstandard interactions in neutrino oscillations and the recent Daya Bay and T2K experiments

Rathin Adhikari,^{1,*} Sabyasachi Chakraborty,^{2,†} Arnab Dasgupta,^{1,‡} and Sourov Roy^{2,§}

¹*Centre for Theoretical Physics, Jamia Millia Islamia (Central University), Jamia Nagar, New Delhi 110025, India*

²*Department of Theoretical Physics, Indian Association for the Cultivation of Science,*

2A & 2B Raja S. C. Mullick Road, Jadavpur, Kolkata 700 032, India

(Received 30 January 2012; published 17 October 2012)

We study the possible constraints on nonstandard interaction (NSIs) in a model-independent way by considering the recent results from the T2K and Daya Bay neutrino oscillations experiments. Using the perturbation method we present generic formulas (suitable for T2K baseline and for large θ_{13} as evident from Daya Bay) for the probability of oscillation for $\nu_\mu \rightarrow \nu_e$, taking into account NSIs at the source (ϵ^s), the detector (ϵ^d), and during propagation (ϵ^m) of neutrinos through matter. Two separate cases of perturbation with small (slightly large) NSI [$\epsilon_{\alpha\beta}^m \sim 0.03(0.18)$] are discussed in detail. Using various possible presently allowed NSI values we reanalyze numerically the $\theta_{13} - \delta$ allowed region given by recent T2K experimental data. We obtain model-independent constraints on NSIs in the $\delta - \epsilon_{\alpha\beta}^m$ plane using the θ_{13} value as measured by Daya Bay, where δ is the CP violating phase. Depending on δ values, significant constraints on $\epsilon_{e\tau}$ and $\epsilon_{\tau\tau}$, in particular, are possible for both hierarchies of neutrino masses. Corresponding to T2K's 66% confidence level result, the constraints on $\epsilon_{\tau\tau}$ are shown to be independent of any δ value.

DOI: [10.1103/PhysRevD.86.073010](https://doi.org/10.1103/PhysRevD.86.073010)

PACS numbers: 13.15.+g, 14.60.Pq, 14.60.St

I. INTRODUCTION

Neutrino oscillations successfully describe neutrino flavor transitions. The recent superbeam and reactor neutrino experiments have provided enormous insights to unravel the exact value of the vacuum mixing angle θ_{13} . To emphasize this point, the T2K [1] experiment observed indications of $\nu_\mu \rightarrow \nu_e$ appearance by producing a conventional neutrino beam at J-PARC and directed 2.5° off axis to a detector situated at 295 Km away. The bounds on θ_{13} that T2K came up with were $0.03(0.04) < \sin^2 2\theta_{13} < 0.28(0.34)$ for $\delta = 0$ and normal (inverted) hierarchy. The reactor neutrino experiments like Daya Bay [2] and Reno [3] provided compelling evidence for a relatively large angle θ_{13} , with 5.2σ and 4.9σ results, respectively. These recent reactor neutrino results indicate θ_{13} very close to 8.8° .

In this work we considered nonstandard interactions (NSIs), occurring from four-fermion operators. In addition to the standard model Lagrangian density, we consider the following nonstandard interactions in the low energy effective theory during the propagation of neutrinos through matter:

$$\mathcal{L}_{\text{NSI}}^M = -2\sqrt{2}G_F \epsilon_{\alpha\beta}^{fP} [\bar{f}\gamma^\mu P f][\bar{\nu}_\alpha \gamma_\mu P_L \nu_\beta], \quad (1)$$

where $f = e, u, d$ and $P = P_L, P_R$ where $P_L = (1 - \gamma_5)/2$ and $P_R = (1 + \gamma_5)/2$. In our subsequent

sections these NSIs are related to $\epsilon_{\alpha\beta}^m$ as mentioned later. In the neutrino oscillation experiments for the NSIs at the source and the detector, the following Lagrangian densities as low energy effective theory corresponding to charged current interactions due to leptons and quarks may be considered:

$$\mathcal{L}_{\text{NSI}}^{S,D} = -2\sqrt{2}G_F \epsilon_{\gamma\delta}^{\lambda\sigma P} [\bar{l}_\lambda \gamma^\mu P l_\sigma][\bar{\nu}_\gamma \gamma_\mu P_L \nu_\delta], \quad (2)$$

$$\mathcal{L}_{\text{NSI}}^{S,D} = -2\sqrt{2}G_F \epsilon_{\gamma\delta}^{udP} V_{ud} [\bar{u}\gamma^\mu P d][\bar{l}_\gamma \gamma_\mu P_L \nu_\delta] + \text{H.c.} \quad (3)$$

In our subsequent sections both these NSIs— $\epsilon_{\gamma\delta}^{\lambda\sigma P}$ and $\epsilon_{\gamma\delta}^{udP}$ contribute to $\epsilon_{\alpha\beta}^s$ and $\epsilon_{\alpha\beta}^d$ corresponding to the appropriate interactions at the source and the detector for the neutrinos, respectively. From the Lagrangian, we observe that the NSI parameters do not possess any mass dimension. However, if NSIs are related to the underlying new physics, then they should be considered as a first-order term in the perturbation series and not in the zeroth order [4]. To reiterate this, we know the NSI parameters are related to the new physics scale in the form $\epsilon \sim (M_W/M_{\text{NSI}})^2$, where M_{NSI} signifies the new physics scale. So if we consider the new physics scale to be around a few TeV, then the NSI parameters should not be greater than a few percent. In general the NSI parameters can be categorized into two different parts. One is the NSI during propagation, and the other being NSI at the source and at the detector. It is worthwhile to note that the present

*rathin@ctp-jamia.res.in

†tpsc3@iacs.res.in

‡arnab@ctp-jamia.res.in

§tpsr@iacs.res.in

bounds on the NSI parameters during propagation are not very stringent [5].

Nonstandard interaction and its implications in a model-independent way, as well as in different models, have already been studied very extensively in the literature [6–18]. Many authors have studied their impact on solar neutrinos [19–22], atmospheric neutrinos [23–28], conventional and upgraded neutrino beams [7,9,17,18,29,30], neutrino factories [7,8,10–12,14,31–33], beta beams [34], supernova neutrinos [35–37], cosmological relic neutrinos [38], and the neutrino-instability problem [39]. Also in some cases similarity of such effective interactions with *CPT* violations [40] and probing such interactions at LHC [41] have been discussed. In the context of solar neutrinos, possible confusion of nonzero mixing angle θ_{13} in the presence of NSI and a hint of NSI have been mentioned [42]. One of the most striking features of NSI parameters is to cloud the sensitivity of θ_{13} by orders of magnitude, which was shown very explicitly in Refs. [13,43], for neutrino factories and reactor neutrino experiments, respectively.

To elaborate the plan of our paper, in Sec. II we present a generalized prescription (suitable for relatively short baseline of T2K) by following the works of Refs. [44–46], which in the literature is also known as the “ $\sqrt{\epsilon}$ method of perturbation theory,” where $\epsilon \equiv \frac{\Delta m_{21}^2}{\Delta m_{31}^2} \sim 0.03$, and we represent a mathematical formulation by considering a relatively large $\sin\theta_{13} \sim \sqrt{\epsilon} \sim 0.18$. We divide the Hamiltonian, consisting of the standard matter interaction and NSI during propagation, into zeroth order part and a perturbative part, where $\sqrt{\epsilon}$ is the perturbation parameter. Our next task is to compute the *S*-matrix elements from these Hamiltonians. In Sec. III, we invoke the idea of NSI parameters at the source and the detector. Previous bounds on these parameters were constrained by lepton and pion decays [10,24], which were of the order of $\mathcal{O}(0.1)$. However, the present bounds on NSI parameters at the source and at the detector are very strong [5]. Because of this reason, we assume the NSI parameters present at the source and the detector are of the order of ϵ . In Secs. IV and V we have considered two different cases, one with the consideration of $\epsilon_{\alpha\beta}^m \sim \sqrt{\epsilon}$ and the other case with $\epsilon_{\alpha\beta}^m \sim \epsilon$, where $\epsilon_{\alpha\beta}^m$ is the NSI parameter during propagation. We have presented the expression of the probability up to second order in ϵ by taking into consideration all these effects, such as the standard matter interaction, NSI during propagation, and NSI at the source and at the detector. We were able to match the results obtained from the analytical expressions with that of the full numerical study. This also shows the remarkable power of this perturbation method. We show that because of the presence of NSIs at the source and at the detector, one can have a nonzero oscillation probability

at the source itself without the neutrino traversing any length. This is coined as the zero distance effect [47–50] or the near detector effect [51] in the literature. This effect is a manifestation of the nonunitarity of the mixing matrix by considering NSIs at the source and at the detector.

It is also important to note that, in principle, one can also follow the method of matrix perturbation to obtain the expression for the probability. In that case one has to compute the modification of the Pontecorvo-Maki-Nakagawa-Sakata (PMNS) matrix [52,53], due to the inclusion of the standard matter interaction and NSI during propagation. The modified PMNS matrix has to be diagonalized; the eigenvectors and the eigenvalues are to be extracted from the modified PMNS matrix. After that NSI at the source and at the detector are to be included, to compute the overall expression of the oscillation probability. Similar approaches were followed by the authors of Refs. [54,55]

In Sec. VI, using Daya Bay and T2K experimental results, we have discussed numerical analysis in obtaining the constraints in the δ -NSI plane. Here, the larger model-independent allowed values of NSI (not considered in our perturbative approach) have been considered for the analysis.

II. MATHEMATICAL FORMULATION FOR LARGE θ_{13} PERTURBATION THEORY

The recent reactor-based neutrino experiments have provided substantial proof for a relatively larger θ_{13} . Based on the works of Refs. [44–46], we describe a mathematical prescription to show the effects of the nonstandard interactions during propagation in neutrino oscillations. We consider the channel $\nu_\mu \rightarrow \nu_e$, as followed by the recently concluded T2K experiment. Using the present experimental values of θ_{13} and the mass squared differences, we formulate

$$\sin\theta_{13} = s_{13} \sim \sqrt{\epsilon}, \quad \epsilon \equiv \frac{\Delta m_{21}^2}{\Delta m_{31}^2} \sim 0.03. \quad (4)$$

This section elaborates the basic principles of our perturbative approach. In the Schrödinger picture, a neutrino with flavor α obeys the evolution equation [56]

$$i \frac{d|\nu_\alpha(t)\rangle}{dt} = \mathcal{H}|\nu_\alpha(t)\rangle; \quad |\nu_\alpha(0)\rangle = |\nu_\alpha\rangle, \quad (5)$$

where the Hamiltonian (after extracting constant diagonal matrix irrelevant for flavor transition as it generates a phase common to all flavors) is given as

$$\mathcal{H} = \frac{1}{2E} \left[U \begin{pmatrix} 0 & 0 & 0 \\ 0 & \Delta m_{21}^2 & 0 \\ 0 & 0 & \Delta m_{31}^2 \end{pmatrix} U^\dagger + A \begin{pmatrix} 1 & 0 & 0 \\ 0 & 0 & 0 \\ 0 & 0 & 0 \end{pmatrix} \right]. \quad (6)$$

The inclusion of the standard matter effect to the Hamiltonian is commonly known as the Mikheyev-Smirnov-Wolfenstein effect [57,58]. Here

$$U = U_{23}U_{13}U_{12} = \begin{bmatrix} 1 & 0 & 0 \\ 0 & c_{23} & s_{23} \\ 0 & -s_{23} & c_{23} \end{bmatrix} \begin{bmatrix} c_{13} & 0 & s_{13}e^{-i\delta} \\ 0 & 1 & 0 \\ -s_{13}e^{i\delta} & 0 & c_{13} \end{bmatrix} \times \begin{bmatrix} c_{12} & s_{12} & 0 \\ -s_{12} & c_{12} & 0 \\ 0 & 0 & 1 \end{bmatrix}, \quad (7)$$

is the PMNS [52,53] matrix in vacuum. $A = 2EV_{cc}$ represents the interaction of the neutrino with matter, more precisely with electrons. E is the energy of the neutrino, V_{cc} represents the charge current interaction and given by $V_{cc} = \sqrt{2}G_F N_e$, where G_F is the Fermi coupling constant and N_e is the electron number density.

By taking Δm_{31}^2 outside the square brackets, from Eq. (6), we redefine the matter interaction as $\hat{A} = A/\Delta m_{31}^2$ and define $\alpha = \frac{\Delta m_{21}^2}{\Delta m_{31}^2} \sim \epsilon$. For the T2K experiment, $\hat{A} = 0.06 \simeq \epsilon$.

From Eq. (6), let us first consider the case where NSI is absent. As a method to simplify calculations, it is convenient to work in the tilde basis, which we define as $\tilde{\nu}_\alpha = (U_{23}^\dagger)_{\alpha\beta} \nu_\beta$. In this basis the Hamiltonian, consisting of only the standard matter interaction part, or \mathcal{H}_M becomes

$$\tilde{\mathcal{H}}_M = U_{23}^\dagger \mathcal{H}_M U_{23}, \quad (8)$$

where we have defined U_{23} in Eq. (7). This Hamiltonian in the tilde basis can now be written as a sum of the Hamiltonians of different orders ($\tilde{\mathcal{H}}_M = \tilde{H}_0 + \tilde{H}_1$), where the ordering is done with respect to $\sqrt{\epsilon}$. For example the zeroth order Hamiltonian, as a function of standard matter interaction looks like,

$$\tilde{H}_0 = \frac{\Delta m_{31}^2}{2E} \begin{bmatrix} 0 & 0 & 0 \\ 0 & 0 & 0 \\ 0 & 0 & 1 \end{bmatrix}, \quad (9)$$

and similarly,

$$\begin{aligned} \tilde{H}_1 = & \frac{\Delta m_{31}^2}{2E} \begin{bmatrix} 0 & 0 & s_{13}e^{-i\delta} \\ 0 & 0 & 0 \\ s_{13}e^{i\delta} & 0 & 0 \end{bmatrix} + \frac{\Delta m_{31}^2}{2E} \begin{bmatrix} \hat{A} + \alpha s_{12}^2 + s_{13}^2 & \alpha c_{12}s_{12} & 0 \\ \alpha c_{12}s_{12} & \alpha c_{12}^2 & 0 \\ 0 & 0 & -s_{13}^2 \end{bmatrix} \\ & - \frac{\Delta m_{31}^2}{2E} \begin{bmatrix} 0 & 0 & (\alpha s_{12}^2 + \frac{1}{2}s_{13}^2)s_{13}e^{-i\delta} \\ 0 & 0 & \alpha c_{12}s_{12}s_{13}e^{-i\delta} \\ (\alpha s_{12}^2 + \frac{1}{2}s_{13}^2)s_{13}e^{i\delta} & \alpha c_{12}s_{12}s_{13}e^{i\delta} & 0 \end{bmatrix} \\ & - \frac{\Delta m_{31}^2}{2E} \alpha \begin{bmatrix} s_{12}^2 s_{13}^2 & \frac{1}{2} c_{12} s_{12} s_{13}^2 & 0 \\ \frac{1}{2} c_{12} s_{12} s_{13}^2 & 0 & 0 \\ 0 & 0 & -s_{12}^2 s_{13}^2 \end{bmatrix}. \end{aligned} \quad (10)$$

Here \tilde{H}_1 is the perturbed part of the Hamiltonian in standard matter. The different matrices in the perturbed Hamiltonian in the tilde basis comprises four different orders in $\sqrt{\epsilon}$, which are $\sqrt{\epsilon}$, ϵ , $\epsilon^{\frac{3}{2}}$, and ϵ^2 , respectively.

Now we include the NSI matrix during propagation. The Hamiltonian consisting of these NSI parameters has the form [4]

$$\mathcal{H}_{\text{NSI}} = \frac{\Delta m_{31}^2}{2E} \hat{A} \begin{bmatrix} \epsilon_{ee}^m & \epsilon_{e\mu}^m & \epsilon_{e\tau}^m \\ \epsilon_{e\mu}^{m*} & \epsilon_{\mu\mu}^m & \epsilon_{\mu\tau}^m \\ \epsilon_{e\tau}^{m*} & \epsilon_{\mu\tau}^{m*} & \epsilon_{\tau\tau}^m \end{bmatrix}, \quad (11)$$

where,

$$\epsilon_{\alpha\beta}^m = \sum_{f,P} \epsilon_{\alpha\beta}^{fP} \frac{n_f}{n_e}, \quad (12)$$

where n_f is the number density of the fermion f [5]. Here $\epsilon_{\alpha\beta}^m$, ($\alpha, \beta = e, \mu, \tau$) are nonstandard interaction parameters of neutrinos, propagating through matter, defined as $\epsilon_{\alpha\beta}^m = |\epsilon_{\alpha\beta}^m| e^{i\phi_{\alpha\beta}}$. To include the \mathcal{H}_{NSI} matrix in the perturbative part of the Hamiltonian, we have to first rotate the \mathcal{H}_{NSI} matrix from its flavor basis to the tilde basis by

$$\tilde{\mathcal{H}}_{\text{NSI}} = U_{23}^\dagger \mathcal{H}_{\text{NSI}} U_{23}. \quad (13)$$

Thus our total Hamiltonian ($\tilde{\mathcal{H}} = \tilde{\mathcal{H}}_M + \tilde{\mathcal{H}}_{\text{NSI}}$) in the tilde basis can be written as a linear superposition of the zeroth order Hamiltonian (\tilde{H}_0) with its perturbative parts in that same basis. After the inclusion of the NSI matrix, which has its effects at the subleading part, we now redefine our Hamiltonian in the perturbative limit as ($\tilde{H}_1 \rightarrow \tilde{H}_1 + \tilde{\mathcal{H}}_{\text{NSI}}$). Because the upper bounds of these NSI parameters are quite high [5], we will consider two different cases, one with $\epsilon_{\alpha\beta}^m \sim \sqrt{\epsilon}$ and the other with $\epsilon_{\alpha\beta}^m \sim \epsilon$. Once we write the Hamiltonian in the tilde basis in this form, we would then look to evaluate the S matrix. The S matrix in the tilde basis is related to the S matrix in the flavor basis by $S(L) = U_{23}\tilde{S}(L)U_{23}^\dagger$, where $\tilde{S}(L) = T \exp[-i \int_0^L dx \tilde{\mathcal{H}}(x)]$ and L is the distance traversed. To evaluate $\tilde{S}(L)$ perturbatively, we choose $\Omega(x)$ as $\Omega(x) = e^{i\tilde{H}_0 x} \tilde{S}(x)$, where $\Omega(x)$ obeys the evolution equation,

$$i \frac{d}{dx} \Omega(x) = H_1 \Omega(x), \quad (14)$$

and H_1 is written in the form

$$H_1 \equiv e^{i\tilde{H}_0 x} \tilde{H}_1 e^{-i\tilde{H}_0 x}. \quad (15)$$

From (14), we would like to deduce $\Omega(x)$ perturbatively. So the solution of the evolution equation followed by $\Omega(x)$, can be written in terms of the H_1 matrices as

$$\begin{aligned} \Omega(x) = & 1 + (-i) \int_0^x dx' H_1(x') + (-i)^2 \int_0^x dx' H_1(x') \\ & \times \int_0^{x'} dx'' H_1(x'') + (-i)^3 \int_0^x dx' H_1(x') \\ & \times \int_0^{x'} dx'' H_1(x'') \int_0^{x''} dx''' H_1(x''') + \mathcal{O}(\epsilon^4). \end{aligned} \quad (16)$$

From our previous definition of $\Omega(x)$, we can now write the S matrix as

$$\tilde{S}(x) = e^{-i\tilde{H}_0 x} \Omega(x). \quad (17)$$

The S matrix in the flavor basis is obtained by rotating \tilde{S} in the (2–3) space as $S = U_{23} \tilde{S} U_{23}^\dagger$.

Since the S matrix changes the flavor of a neutrino state after traversing a length L , which is given by the expression

$$\nu_\alpha(L) = S_{\alpha\beta} \nu_\beta(0), \quad (18)$$

the oscillation probability of the neutrino, changing the flavor from $\alpha \rightarrow \beta$, is given as

$$P(\nu_\beta \rightarrow \nu_\alpha; L) = |S_{\alpha\beta}|^2. \quad (19)$$

This expression of the oscillation probability takes into consideration the standard matter interaction and the NSI during propagation only. In Sec. III we will introduce the idea of NSI at the source and the detector.

It should be noted that since θ_{12} and θ_{23} are quite large, compared to θ_{13} , they are considered to be in the zeroth order.

III. NSI AT SOURCE, DETECTOR, AND DURING PROPAGATION IN $\nu_\mu \rightarrow \nu_e$ OSCILLATION PROBABILITY

In the presence of NSI at the source and at the detector, the neutrino states produced at the detector can be treated as a superposition [43,59] of pure orthonormal flavor states,

$$|\nu_\alpha^s\rangle = \frac{1}{N_\alpha^s} \left(|\nu_\alpha\rangle + \sum_{\beta=e,\mu,\tau} \epsilon_{\alpha\beta}^s |\nu_\beta\rangle \right), \quad (20)$$

$$\langle \nu_\beta^d | = \frac{1}{N_\beta^d} \left(\langle \nu_\beta | + \sum_{\alpha=e,\mu,\tau} \epsilon_{\alpha\beta}^d \langle \nu_\alpha | \right), \quad (21)$$

where, $\epsilon_{\alpha\beta}^s$ and $\epsilon_{\alpha\beta}^d$ are NSI at the source and the detector, respectively, and the normalization factors are given by

$$\begin{aligned} N_\alpha^s &= \sqrt{[(\mathbf{1} + \epsilon^s)(\mathbf{1} + \epsilon^{s\dagger})]_{\alpha\alpha}}, \\ N_\beta^d &= \sqrt{[(\mathbf{1} + \epsilon^{d\dagger})(\mathbf{1} + \epsilon^d)]_{\beta\beta}}. \end{aligned} \quad (22)$$

For example, $\epsilon_{\alpha\beta}^s$ describes a nonstandard admixture of flavor β to the neutrino state that is produced in association with a charged lepton of flavor α . This means the neutrino source does not produce a pure flavor neutrino eigenstate $|\nu_\alpha\rangle$ but rather a superposition of pure orthonormal flavor states [51]. To be consistent with the literature the convention that we have chosen is in $\epsilon_{\alpha\beta}^s$, the first index corresponds to the flavor of the charged lepton, and the second to that of the neutrino, while in $\epsilon_{\alpha\beta}^d$, the order is reversed. In general, as we can clearly see from the definitions above, the matrices $(\mathbf{1} + \epsilon^s)$ and $(\mathbf{1} + \epsilon^d)$ are nonunitary, i.e., the source and the detection states do not require one to form a complete orthonormal sets of basis vectors in the Hilbert space.

Since the coefficients $\epsilon_{e\alpha}^s$ and $\epsilon_{\alpha e}^d$ both originate from the $(V - A)(V \pm A)$ coupling [51] to up and down quarks, we have the constraint

$$\epsilon_{e\alpha}^s = \epsilon_{\alpha e}^{d*}. \quad (23)$$

Thus this condition reduces the number of independent parameters and makes the model more predictive. But in our paper we have presented the most general case.

Considering the NSI effects at the source and the detector, as well as during the propagation of neutrinos through matter, the amplitude of the oscillation becomes

$$\begin{aligned}
P_{\nu_\alpha^s \rightarrow \nu_\beta^d} &= |\langle \nu_\beta^d | S(L) | \nu_\alpha^s \rangle|^2 \\
&= \left| \frac{1}{N_\alpha^s N_\beta^d} (1 + \epsilon^d)_{\gamma\beta} (S(L))_{\gamma\delta} (1 + \epsilon^s)_{\alpha\delta} \right|^2 \\
&= \left| \frac{1}{N_\alpha^s N_\beta^d} [(1 + \epsilon^d)^T S(L) (1 + \epsilon^s)^T]_{\beta\alpha} \right|^2, \quad (24)
\end{aligned}$$

where the $S(L)$ is defined earlier. Considering NSI at the source and at the detector of the order of ϵ [5], we can now write the probability expression as a sum of the probabilities of different order $\sqrt{\epsilon}$ terms. The total oscillation probability would look like

$$P(\nu_\alpha \rightarrow \nu_\beta) = P_{\alpha\beta}^{(0)} + P_{\alpha\beta}^{(1/2)} + P_{\alpha\beta}^{(1)} + P_{\alpha\beta}^{(3/2)} + P_{\alpha\beta}^{(2)} \quad (25)$$

In our later analysis we would incorporate the results from the reactor neutrino experiments along with the long baseline superbeam experiment such as T2K. It is notable that the nonstandard interaction parameters during propagation do not play any substantial role in case of the reactor neutrino experiments, due to its very short baseline. Furthermore, the NSI parameters present both at the source and at the detector of these two different kinds of neutrino experiments, i.e., $\epsilon_{\alpha\beta}^s$ and $\epsilon_{\alpha\beta}^d$, are considered to be the same. The oscillation probability $P(\nu_\alpha \rightarrow \nu_\beta)$ is for a neutrino, rather than an antineutrino. However, one can relate the oscillation probabilities for antineutrinos to those for neutrinos by

$$P_{\bar{\alpha}\bar{\beta}} = P_{\alpha\beta}(\delta_{CP} \rightarrow -\delta_{CP}, \hat{A} \rightarrow -\hat{A}). \quad (26)$$

In addition, we also have to replace ϵ^s , ϵ^d , $\epsilon_{\alpha\beta}^m$ with their complex conjugates, in order to deduce the oscillation

probability for the antineutrino, if one considers nonstandard interaction during propagation and at the source and the detector of the experiment.

It should be noted that the expression (24) is also valid in the minimal unitarity violation model and is very instructive for analyzing the CP violating effects in the minimal unitarity violation model in future long baseline experiments [47,48,60–64].

IV. PERTURBATION THEORY BY CONSIDERING LARGE NSI PARAMETERS DURING PROPAGATION

In our next two sections, we will consider two different cases of these NSI parameters and present oscillation probability for the channel $\nu_\mu \rightarrow \nu_e$, as was observed by the T2K experiment. In this section, we will consider $\epsilon_{\alpha\beta}^m \sim \sqrt{\epsilon} \sim 0.18$, and in the next section we will put $\epsilon_{\alpha\beta}^m \sim \epsilon \sim 0.03$.

Since \hat{A} is of the order of ϵ , \mathcal{H}_{NSI} is in the perturbative range $\epsilon^{\frac{3}{2}}$. Furthermore, we also have to transform \mathcal{H}_{NSI} from its flavor basis to the tilde basis, e.g.,

$$\tilde{\mathcal{H}}_{\text{NSI}} = U_{23}^\dagger \mathcal{H}_{\text{NSI}} U_{23}. \quad (27)$$

Our total Hamiltonian now looks like

$$\tilde{\mathcal{H}} = \tilde{H}_0 + [\tilde{H}_1 + \tilde{\mathcal{H}}_{\text{NSI}}]. \quad (28)$$

We include this $\tilde{\mathcal{H}}_{\text{NSI}}$ in the perturbative part of the Hamiltonian and follow the same calculations described previously. The order $\epsilon^{3/2}$ component of the Hamiltonian now looks like

$$\begin{aligned}
\tilde{H}_1(\epsilon^{3/2}) &= -\frac{\Delta m_{31}^2}{2E} s_{13} \begin{bmatrix} 0 & 0 & (\alpha s_{12}^2 + \frac{1}{2} s_{13}^2) e^{-i\delta} \\ 0 & 0 & \alpha c_{12} s_{12} e^{-i\delta} \\ (\alpha s_{12}^2 + \frac{1}{2} s_{13}^2) e^{i\delta} & \alpha c_{12} s_{12} e^{i\delta} & 0 \end{bmatrix} \\
&+ \frac{\Delta m_{31}^2}{2E} \hat{A} U_{23}^\dagger \begin{bmatrix} \epsilon_{ee}^m & \epsilon_{e\mu}^m & \epsilon_{e\tau}^m \\ \epsilon_{e\mu}^{m*} & \epsilon_{\mu\mu}^m & \epsilon_{\mu\tau}^m \\ \epsilon_{e\tau}^{m*} & \epsilon_{\mu\tau}^{m*} & \epsilon_{\tau\tau}^m \end{bmatrix} U_{23}. \quad (29)
\end{aligned}$$

By computing the S matrix, which comprises the standard matter interaction and NSI during propagation of the neutrino, we then include the NSI parameters at the source and the detector, which are of the order of ϵ , as per the present bounds on these parameters suggest. Finally we write down the oscillation probability for the muon neutrino going to electron neutrino up to second order in ϵ . It is noteworthy that due to the nonunitarity of the nonstandard interaction matrices at the source and at the detector, the

probability of neutrino oscillation is not normalized to unity. So one has to include necessary normalization factors as we have done in (22). In the context of T2K, where we are observing muon neutrino oscillation to electron neutrino, these normalization factors do not play a very significant role. To be precise, the effects of these normalization terms are greater than $\mathcal{O}(\epsilon^2)$, which we are neglecting. Finally by considering all these effects, the oscillation probability in the $\nu_\mu \rightarrow \nu_e$ channel is,

$$\begin{aligned}
P_{\nu_\mu \rightarrow \nu_e} = & |\epsilon_{e\mu}^d|^2 + |\epsilon_{e\mu}^s|^2 + 2|\epsilon_{e\mu}^d||\epsilon_{e\mu}^s| \cos[\phi_{e\mu}^d - \phi_{e\mu}^s] + \frac{L^2 \alpha^2 \Delta m_{31}^4 c_{23}^2 s_{2 \times 12}^2}{16E^2} + \frac{L\alpha \Delta m_{31}^2 |\epsilon_{e\tau}^d| c_{23}^2}{E} \cos\left[\frac{L\Delta m_{31}^2}{4E} + \phi_{e\tau}^d\right] \\
& \times \sin\left[\frac{L\Delta m_{31}^2}{4E}\right] s_{2 \times 12} s_{23} - 2|\epsilon_{e\mu}^d||\epsilon_{e\mu}^s| \cos[\phi_{e\mu}^d] \cos[\phi_{e\mu}^s] s_{23}^2 + 2|\epsilon_{e\mu}^d||\epsilon_{e\mu}^s| \cos\left[\frac{L\Delta m_{31}^2}{2E}\right] \cos[\phi_{e\mu}^d] \cos[\phi_{e\mu}^s] s_{23}^2 \\
& + 8a_3 \cos[\delta + \phi_{a_3}] \sin^2\left[\frac{L\Delta m_{31}^2}{4E}\right] s_{13} s_{23}^2 + 8|\epsilon_{ee}^d| \sin^2\left[\frac{L\Delta m_{31}^2}{4E}\right] s_{13}^2 s_{23}^2 + 8|\epsilon_{\mu\mu}^s| \sin^2\left[\frac{L\Delta m_{31}^2}{4E}\right] s_{13}^2 s_{23}^2 + \frac{s_{13}^2 s_{23}^2}{E} \\
& \times \sin\left[\frac{L\Delta m_{31}^2}{4E}\right] \left(-2AL\Delta m_{31}^2 \cos\left[\frac{L\Delta m_{31}^2}{4E}\right] + 2E(1 + 4A + c_{2 \times 13}) \sin\left[\frac{L\Delta m_{31}^2}{4E}\right]\right) + 4|\epsilon_{e\tau}^d| c_{23} \sin^2\left[\frac{L\Delta m_{31}^2}{4E}\right] \\
& \times (|\epsilon_{e\tau}^d| c_{23} + 2 \cos[\delta - \phi_{e\tau}^d] s_{13}) s_{23}^2 + \frac{L\alpha \Delta m_{31}^2 s_{13} s_{23}}{E} \left(\cos\left[\delta + \frac{L\Delta m_{31}^2}{4E}\right] c_{23} \sin\left[\frac{L\Delta m_{31}^2}{4E}\right] s_{2 \times 12} \right. \\
& \left. - \sin\left[\frac{L\Delta m_{31}^2}{2E}\right] s_{12}^2 s_{13} s_{23}\right) + \frac{a_2 L \Delta m_{31}^2}{E} \cos\left[\delta + \frac{L\Delta m_{31}^2}{4E} + \phi_{a_2}\right] \sin\left[\frac{L\Delta m_{31}^2}{4E}\right] s_{13} s_{2 \times 23} - 2|\epsilon_{e\mu}^d||\epsilon_{e\tau}^d| \\
& \times \sin\left[\frac{L\Delta m_{31}^2}{4E}\right] s_{2 \times 23} \left(c_{2 \times 23} \cos[\phi_{e\tau}^d - \phi_{e\mu}^d] \sin\left[\frac{L\Delta m_{31}^2}{4E}\right] + \cos\left[\frac{L\Delta m_{31}^2}{4E}\right] \sin[\phi_{e\tau}^d - \phi_{e\mu}^d]\right) \\
& - 2|\epsilon_{e\mu}^d||\epsilon_{e\mu}^s| \cos[\phi_{e\mu}^s] \sin\left[\frac{L\Delta m_{31}^2}{2E}\right] s_{23}^2 \sin[\phi_{e\mu}^d] - 2s_{23} \left(|\epsilon_{e\mu}^d| \cos[\phi_{e\mu}^d] \sin[\delta] \sin\left[\frac{L\Delta m_{31}^2}{2E}\right] s_{13} \right. \\
& \left. + |\epsilon_{e\mu}^d| \cos[\delta] s_{13} \left(2c_{2 \times 23} \cos[\phi_{e\mu}^d] \sin^2\left[\frac{L\Delta m_{31}^2}{4E}\right] - \sin\left[\frac{L\Delta m_{31}^2}{2E}\right] \sin[\phi_{e\mu}^d]\right) + 2\sin^2\left[\frac{L\Delta m_{31}^2}{4E}\right] \right) \\
& \times \left(-2|\epsilon_{\mu\tau}^s| c_{23} \cos[\phi_{\mu\tau}^s] s_{13}^2 + |\epsilon_{e\mu}^d|^2 c_{23}^2 s_{23} + |\epsilon_{e\mu}^d| c_{2 \times 23} \sin[\delta] s_{13} \sin[\phi_{e\mu}^d]\right) + \frac{L\alpha \Delta m_{31}^2 |\epsilon_{e\mu}^d| c_{23} s_{2 \times 12}}{2E} \\
& \times \left(c_{23}^2 \sin[\phi_{e\mu}^d] + s_{23}^2 \sin\left[\frac{L\Delta m_{31}^2}{2E} + \phi_{e\mu}^d\right]\right) - 4|\epsilon_{e\mu}^s| \sin\left[\frac{L\Delta m_{31}^2}{4E}\right] s_{13} s_{23} \sin\left[\delta + \frac{L\Delta m_{31}^2}{4E} - \phi_{e\mu}^s\right] \\
& - 2|\epsilon_{e\tau}^d||\epsilon_{e\mu}^s| \sin\left[\frac{L\Delta m_{31}^2}{4E}\right] s_{2 \times 23} \sin\left[\frac{L\Delta m_{31}^2}{4E} + \phi_{e\tau}^d - \phi_{e\mu}^s\right] + \frac{L\alpha \Delta m_{31}^2 |\epsilon_{e\mu}^s| c_{12} c_{23} s_{12}}{E} \sin[\phi_{e\mu}^s] \\
& + 2|\epsilon_{e\mu}^d||\epsilon_{e\mu}^s| \cos[\phi_{e\mu}^d] \sin\left[\frac{L\Delta m_{31}^2}{2E}\right] s_{23}^2 \sin[\phi_{e\mu}^s] - 2|\epsilon_{e\mu}^d||\epsilon_{e\mu}^s| s_{23}^2 \sin[\phi_{e\mu}^d] \sin[\phi_{e\mu}^s] \\
& + 2|\epsilon_{e\mu}^d||\epsilon_{e\mu}^s| \cos\left[\frac{L\Delta m_{31}^2}{2E}\right] s_{23}^2 \sin[\phi_{e\mu}^d] \sin[\phi_{e\mu}^s], \tag{30}
\end{aligned}$$

where $s_{2 \times ij} = \sin 2\theta_{ij}$ and $c_{2 \times ij} = \cos 2\theta_{ij}$ and

$$\begin{aligned}
a_2 &= \frac{A}{\sqrt{2}} \sqrt{|\epsilon_{e\mu}^m|^2 + |\epsilon_{e\tau}^m|^2 + (|\epsilon_{e\mu}^m|^2 - |\epsilon_{e\tau}^m|^2) c_{2 \times 23} - 2|\epsilon_{e\mu}^m||\epsilon_{e\tau}^m| \cos[\phi_{e\mu}^m - \phi_{e\tau}^m] s_{2 \times 23}}, \\
a_3 &= \frac{A}{\sqrt{2}} \sqrt{|\epsilon_{e\mu}^m|^2 + |\epsilon_{e\tau}^m|^2 + (-|\epsilon_{e\mu}^m|^2 + |\epsilon_{e\tau}^m|^2) c_{2 \times 23} + 2|\epsilon_{e\mu}^m||\epsilon_{e\tau}^m| \cos[\phi_{e\mu}^m - \phi_{e\tau}^m] s_{2 \times 23}}, \\
\phi_{a_2} &= \tan^{-1} \left[\frac{\epsilon_{e\mu}^m c_{23} \sin[\phi_{e\mu}^m] - \epsilon_{e\tau}^m s_{23} \sin[\phi_{e\tau}^m]}{\epsilon_{e\mu}^m c_{23} \cos[\phi_{e\mu}^m] - \epsilon_{e\tau}^m \cos[\phi_{e\tau}^m] s_{23}} \right], \quad \phi_{a_3} = \tan^{-1} \left[\frac{\epsilon_{e\mu}^m s_{23} \sin[\phi_{e\mu}^m] + \epsilon_{e\tau}^m c_{23} \sin[\phi_{e\tau}^m]}{\epsilon_{e\tau}^m c_{23} \cos[\phi_{e\tau}^m] + \epsilon_{e\mu}^m \cos[\phi_{e\mu}^m] s_{23}} \right]. \tag{31}
\end{aligned}$$

There are a few salient features of this expression of the probability. These are as follows:

- (i) Considering the baseline length to be zero, we are left with the term

$$P_{\nu_\mu \rightarrow \nu_e}^{ND} = |\epsilon_{e\mu}^d|^2 + |\epsilon_{e\mu}^s|^2 + 2|\epsilon_{e\mu}^d||\epsilon_{e\mu}^s| \cos(\phi_{e\mu}^d - \phi_{e\mu}^s). \tag{32}$$

This term is the manifestation of the nonunitarity of the source and detector matrices, more commonly known as the zero distance effect.

- (ii) Assuming the standard matter interaction and NSI during the propagation as well as at the source and at the detector to be absent, we can obtain the expression of the probability, representing the vacuum oscillation probability for a three-flavor neutrino scenario correct up to $\mathcal{O}(\alpha^2)$ —particularly, the following leading term of vacuum oscillation [65]

$$P_{\nu_\mu \rightarrow \nu_e}^{\text{Vacuum}} = s_{2 \times 13}^2 s_{23}^2 \sin^2 \left[\frac{\Delta m_{31}^2 L}{4E} \right], \quad (33)$$

can be obtained from the eleventh term of (30) after considering $A \rightarrow 0$.

- (iii) Since muon is produced at the source, we observe only $\epsilon_{e\mu}^s, \epsilon_{\mu\mu}^s, \epsilon_{\mu\tau}^s$ NSI parameters, and the electron is obtained at the detector, thus we observe $\epsilon_{ee}^d, \epsilon_{e\mu}^d, \epsilon_{e\tau}^d$ in our expression for the probability.
- (iv) For the $\nu_\mu \rightarrow \nu_e$ channel, only $\epsilon_{e\mu}^m$ and $\epsilon_{e\tau}^m$ appear as NSI parameters during the propagation of the neutrino. The contribution from all the other NSI parameters during propagation are very much suppressed.
- (v) As mentioned earlier, our expression of the probability is of the order of ϵ^2 , by considering large angle θ_{13} . Similar expressions are to be found in Ref. [51] where the authors considered small θ_{13} . But the recent reactor-based experiments [2,3] compelled us to consider the regime of large $\sin\theta_{13} \sim \sqrt{\epsilon}$.

V. PERTURBATION THEORY BY CONSIDERING SMALL NSI PARAMETERS DURING PROPAGATION

In this section we will concentrate on the idea of small nonstandard interaction parameters during propagation. The standard matter interaction is again considered to be of the order of ϵ , and we now consider NSI during propagation $\epsilon_{\alpha\beta}^m \sim \epsilon$. Following the same argument, as done in the previous section, the zeroth order Hamiltonian in the tilde basis remains the same. However the perturbative Hamiltonian gets rearranged. In this case $\tilde{\mathcal{H}}_{\text{NSI}}$ would be of the order of ϵ^2 .

The ϵ^2 part of the perturbed Hamiltonian (10) can now be written as

$$\tilde{H}_1(\epsilon^2) = -\frac{\Delta m_{31}^2}{2E} \alpha \begin{bmatrix} s_{12}^2 s_{13}^2 & \frac{1}{2} c_{12} s_{12} s_{13}^2 & 0 \\ \frac{1}{2} c_{12} s_{12} s_{13}^2 & 0 & 0 \\ 0 & 0 & -s_{12}^2 s_{13}^2 \end{bmatrix} + \frac{\Delta m_{31}^2}{2E} \hat{A} U_{23}^\dagger \begin{bmatrix} \epsilon_{ee}^m & \epsilon_{e\mu}^m & \epsilon_{e\tau}^m \\ \epsilon_{e\mu}^{m*} & \epsilon_{\mu\mu}^m & \epsilon_{\mu\tau}^m \\ \epsilon_{e\tau}^{m*} & \epsilon_{\mu\tau}^{m*} & \epsilon_{\tau\tau}^m \end{bmatrix} U_{23}. \quad (34)$$

We again follow the same procedure as performed in the previous section. We computed the S matrix, after including the standard matter interaction and NSI during propagation. Then we considered the source and the detector effect. Thus the probability for a muon neutrino going to an electron neutrino for $\epsilon_{\alpha\beta}^m \sim \epsilon$ is given by

$$\begin{aligned} P_{\nu_\mu \rightarrow \nu_e} &= |\epsilon_{e\mu}^d|^2 + |\epsilon_{e\mu}^s|^2 + 2|\epsilon_{e\mu}^d||\epsilon_{e\mu}^s| \cos[\phi_{e\mu}^d - \phi_{e\mu}^s] + \frac{L^2 \alpha^2 \Delta m_{31}^4 c_{23}^2 s_{2 \times 12}^2}{16E^2} + \frac{L\alpha \Delta m_{31}^2 |\epsilon_{e\tau}^d| c_{23}^2}{E} \cos\left[\frac{L\Delta m_{31}^2}{4E} + \phi_{e\tau}^d\right] \\ &\times \sin\left[\frac{L\Delta m_{31}^2}{4E}\right] s_{2 \times 12} s_{23} - 2|\epsilon_{e\mu}^d||\epsilon_{e\mu}^s| \cos[\phi_{e\mu}^d] \cos[\phi_{e\mu}^s] s_{23}^2 + 2|\epsilon_{e\mu}^d||\epsilon_{e\mu}^s| \cos\left[\frac{L\Delta m_{31}^2}{2E}\right] \cos[\phi_{e\mu}^d] \cos[\phi_{e\mu}^s] s_{23}^2 \\ &+ 8|\epsilon_{ee}^d| \sin^2\left[\frac{L\Delta m_{31}^2}{4E}\right] s_{13}^2 s_{23}^2 + 8|\epsilon_{\mu\mu}^s| \sin^2\left[\frac{L\Delta m_{31}^2}{4E}\right] s_{13}^2 s_{23}^2 + \frac{s_{13}^2 s_{23}^2}{E} \sin\left[\frac{L\Delta m_{31}^2}{4E}\right] \left(-2AL\Delta m_{31}^2 \cos\left[\frac{L\Delta m_{31}^2}{4E}\right]\right. \\ &+ 2E(1 + 4A + c_{2 \times 13}) \sin\left[\frac{L\Delta m_{31}^2}{4E}\right]) + 4|\epsilon_{e\tau}^d| c_{23} \sin^2\left[\frac{L\Delta m_{31}^2}{4E}\right] (|\epsilon_{e\tau}^d| c_{23} + 2\cos[\delta - \phi_{e\tau}^d] s_{13}) s_{23}^2 \\ &+ \frac{L\alpha \Delta m_{31}^2 s_{13} s_{23}}{E} \left(\cos\left[\delta + \frac{L\Delta m_{31}^2}{4E}\right] c_{23} \sin\left[\frac{L\Delta m_{31}^2}{4E}\right] s_{2 \times 12} - \sin\left[\frac{L\Delta m_{31}^2}{2E}\right] s_{12}^2 s_{13} s_{23}\right) - 2|\epsilon_{e\mu}^d||\epsilon_{e\tau}^d| \sin\left[\frac{L\Delta m_{31}^2}{4E}\right] \\ &\times s_{2 \times 23} \left(c_{2 \times 23} \cos[\phi_{e\tau}^d - \phi_{e\mu}^d] \sin\left[\frac{L\Delta m_{31}^2}{4E}\right] + \cos\left[\frac{L\Delta m_{31}^2}{4E}\right] \sin[\phi_{e\tau}^d - \phi_{e\mu}^d]\right) - 2|\epsilon_{e\mu}^d||\epsilon_{e\mu}^s| \cos[\phi_{e\mu}^s] \\ &\times \sin\left[\frac{L\Delta m_{31}^2}{2E}\right] s_{23}^2 \sin[\phi_{e\mu}^d] - 2s_{23} \left(|\epsilon_{e\mu}^d| \cos[\phi_{e\mu}^d] \sin[\delta] \sin\left[\frac{L\Delta m_{31}^2}{2E}\right] s_{13} + |\epsilon_{e\mu}^d| \cos[\delta] s_{13} \left(2c_{2 \times 23} \cos[\phi_{e\mu}^d]\right.\right. \\ &\times \sin^2\left[\frac{L\Delta m_{31}^2}{4E}\right] - \sin\left[\frac{L\Delta m_{31}^2}{2E}\right] \sin[\phi_{e\mu}^d]) + 2\sin^2\left[\frac{L\Delta m_{31}^2}{4E}\right] \left(-2|\epsilon_{\mu\tau}^s| c_{23} \cos[\phi_{\mu\tau}^s] s_{13}^2 + |\epsilon_{e\mu}^d|^2 c_{23}^2 s_{23}\right. \\ &+ |\epsilon_{e\mu}^d| c_{2 \times 23} \sin[\delta] s_{13} \sin[\phi_{e\mu}^d]) + \frac{L\alpha \Delta m_{31}^2 |\epsilon_{e\mu}^d| c_{23} s_{2 \times 12}}{2E} \left(c_{23}^2 \sin[\phi_{e\mu}^d] + s_{23}^2 \sin\left[\frac{L\Delta m_{31}^2}{2E} + \phi_{e\mu}^d\right]\right) \\ &- 4|\epsilon_{e\mu}^s| \sin\left[\frac{L\Delta m_{31}^2}{4E}\right] s_{13} s_{23} \sin\left[\delta + \frac{L\Delta m_{31}^2}{4E} - \phi_{e\mu}^s\right] - 2|\epsilon_{e\tau}^d||\epsilon_{e\mu}^s| \sin\left[\frac{L\Delta m_{31}^2}{4E}\right] s_{2 \times 23} \sin\left[\frac{L\Delta m_{31}^2}{4E} + \phi_{e\tau}^d - \phi_{e\mu}^s\right] \\ &+ \frac{L\alpha \Delta m_{31}^2 |\epsilon_{e\mu}^s| c_{12} c_{23} s_{12} \sin[\phi_{e\mu}^s]}{E} + 2|\epsilon_{e\mu}^d||\epsilon_{e\mu}^s| \cos[\phi_{e\mu}^d] \sin\left[\frac{L\Delta m_{31}^2}{2E}\right] s_{23}^2 \sin[\phi_{e\mu}^s] - 2|\epsilon_{e\mu}^d||\epsilon_{e\mu}^s| s_{23}^2 \sin[\phi_{e\mu}^d] \\ &\times \sin[\phi_{e\mu}^s] + 2|\epsilon_{e\mu}^d||\epsilon_{e\mu}^s| \cos\left[\frac{L\Delta m_{31}^2}{2E}\right] s_{23}^2 \sin[\phi_{e\mu}^d] \sin[\phi_{e\mu}^s]. \quad (35) \end{aligned}$$

We would again try to emphasize some of the interesting features about this oscillation probability expression.

- (i) As expected, we get back the same expression for the near detector effect, which was provided in the expression (32).
- (ii) Similar to the result of the previous section, assuming the standard matter interaction and NSI during the propagation as well as at the source and at the detector to be absent, we can obtain the expression of the probability, representing the vacuum oscillation probability for a three-flavor neutrino scenario correct up to $\mathcal{O}(\alpha^2)$. Particularly from the tenth term in (35) considering $A \rightarrow 0$ one can get the leading vacuum oscillation probability in (33).
- (iii) It is very much interesting to note that due to the choice of the NSI parameters during propagation proportional to ϵ , the probability expression up to second order in ϵ for this particular channel is devoid of any terms containing this kind of NSI. It shows that it is very difficult to constrain such small NSIs in relatively short baseline neutrino oscillation experiments like T2K.
- (iv) It is conspicuous that the NSI parameters at the source and at the detector carry the same flavor indices, as in Eq. (30).

VI. NUMERICAL ANALYSIS

Here, we discuss the approach of our complete numerical analysis in obtaining the results presented in this paper giving constraints on NSIs. In our numerical analysis we have considered even much higher values of NSI that have not been considered in our perturbative approach but which are allowed after considering model-independent constraints [5]. Some of the NSIs like ϵ_{ee} , $\epsilon_{\mu\mu}$, $\epsilon_{\tau\tau}$ (for propagation) etc. do not appear in our expression of $P_{\nu_\mu \rightarrow \nu_e}$ in Secs. IV and V as those have been assumed to be very small. In our numerical analysis, however, we still have obtained some constraints on those NSIs because of their presently allowed higher model-independent values as discussed later.

For ultrarelativistic neutrinos, we have

$$E_k \simeq E + \frac{m_k^2 c^4}{2E}, \quad pc \simeq E, \quad ct \simeq x, \quad (36)$$

where $k = 1, 2, 3$ corresponds to mass eigenstates and E_k are the eigenenergies. The neutrino energy E is the average energy after assuming the three momentum of different components (1, 2, and 3) to be equal.

Therefore, for the numerical analysis the relevant transition evolution equation for the flavor transition is

$$i\hbar c \frac{d}{dx} S_{\beta\alpha}(x) = \sum_{\eta} \mathcal{H}_{\beta\eta} S_{\eta\alpha}, \quad (37)$$

with initial condition $S_{\beta\alpha}(0) = \delta_{\beta\alpha}$, and \mathcal{H} is the total Hamiltonian comprising of standard matter interaction and

NSI during propagation. However, here apart from NSI in propagation we want to include the source and the detector NSI interaction. So, to implement that we apply the source and detector NSI matrices to the $S_{\alpha\beta}$ that is already mentioned in (24) as

$$\mathcal{A}_{\beta\alpha} = \frac{1}{N_{\alpha}^s N_{\beta}^d} [(1 + \epsilon^d)^T S (1 + \epsilon^s)^T]_{\beta\alpha}.$$

The probability expression for the transition $\nu_{\alpha} \rightarrow \nu_{\beta}$ is

$$P_{\nu_{\alpha} \rightarrow \nu_{\beta}} = |\mathcal{A}_{\beta\alpha}|^2. \quad (38)$$

Although NSI is considered at the source, that at the detector and that during propagation are in general different. However, following Ref. [43] we have considered $\epsilon_{\alpha\beta}^s = \epsilon_{\beta\alpha}^{d*}$.

The recent T2K result [1] has obtained the constraint on the $\delta - \sin^2 2\theta_{13}$ plane at 90% confidence level based on the events in the $\nu_{\mu} \rightarrow \nu_e$ transition in the baseline of 295 Km. Furthermore, the Daya Bay reactor neutrino experiment has recently measured the neutrino mixing angle θ_{13} with 5.2σ confidence level for which $\sin^2 2\theta_{13} = 0.092 \pm 0.016 \pm 0.005(\text{syst})$. Here, we analyze both of these constraints considering real NSIs (one at a time) in propagation. Somewhat conservative bounds on all NSIs at the source and the detector have been considered and taken to be of about 10^{-3} . To tune with the experimental result of T2K and Daya Bay, we shall use the same range of probability of oscillation as one obtains using the constraints on $\delta - \sin^2 2\theta_{13}$ given by T2K (without considering NSI) at different confidence level for normal and inverted hierarchies (allowing the variation of θ_{13} as in T2K paper). After that we shall fix θ_{13} at the Daya Bay value and find out the allowed ranges in the parameters δ and different NSIs in matter (one at a time) subject to this constraint on the probability of oscillation. For numerical analysis we use the following values as considered by T2K [1]: $\Delta m_{12}^2 = 7.6 \times 10^{-5} \text{ eV}^2$, $\Delta m_{23}^2 = 2.4 \times 10^{-3} \text{ eV}^2$, $\sin^2 2\theta_{12} = 0.8704$, $\sin^2 2\theta_{23} = 1.0$, an average earth density $\rho = 3.2 \text{ g/cm}^3$, and central value of $\sin^2 2\theta_{13} = 0.092$ as obtained from Daya Bay. One may note here that in the presence of NSIs particularly in matter (which are expected to be much larger than those NSIs at the source and the detector) the neutrino mixing parameters considered by T2K could change [66,67]. However, it is found that only when several NSIs are considered simultaneously small changes occur in the best-fit values of these parameters. As for example, considering solar and KamLAND data the change in best-fit value of θ_{12} and Δm_{12}^2 can be seen in Fig. 2 in Ref. [66], and considering atmospheric and K2K data the change in best-fit value of θ_{23} and Δm_{23}^2 can be seen in Fig. 5 in Ref. [67] after considering NSIs like ϵ_{ee} , $\epsilon_{e\tau}$ and $\epsilon_{\tau\tau}$ simultaneously. However, in our analysis, we have obtained a constraint on the δ -NSI plane by considering one of the NSIs at a time for which the changes in these

mixing parameters are expected to be small, and in this simple analysis we use the values of mixing parameters as considered by T2K. For a very rigorous analysis in obtaining these mixing parameters in the presence of NSIs, one is required to fit the solar, KamLAND, atmospheric, and K2K data simultaneously by considering NSIs one at a time or altogether in the general three-flavor neutrino mixing scenario that has not been done so far to the best of our knowledge.

In all the plots of NSI versus δ the $\epsilon_{\alpha\beta}$ corresponds to $\epsilon_{\alpha\beta}^m$ that are NSIs in matter during propagation. Dark shaded regions correspond to the allowed region. The T2K constraint on the $\delta - \sin^2 2\theta_{13}$ plane at 66% confidence level (C.L.) together with Daya Bay result in θ_{13} corresponding to the excluded region (white + grey) and only the white excluded region corresponds to the same T2K constraint at 90% C.L. We have done the analysis

on NSI constraints keeping in view the allowed range of NSIs for earthlike matters as mentioned in Ref. [5] and have considered those for real values. The upper (lower) panel in each plot corresponds to normal (inverted) hierarchies. Out of various NSIs the significant constraints are obtained particularly for $\epsilon_{e\tau}^m$ and $\epsilon_{\tau\tau}^m$ for both the hierarchies of neutrino masses. Particularly for $\epsilon_{\mu\mu}$ and $\epsilon_{\mu\tau}$ no constraint can be obtained for normal hierarchy.

In Fig. 1 it is seen that in the upper panel for normal hierarchy the constraints on ϵ_{ee} can be obtained for negative values only for certain values of δ corresponding to T2K's 66% confidence level result whereas for inverted hierarchy the constraint is mainly on positive ϵ_{ee} . However, for inverted hierarchy there is also an excluded white region corresponding to T2K's 90% confidence level result. In Fig. 2 the constraint on $\epsilon_{e\mu}$ is found mainly for

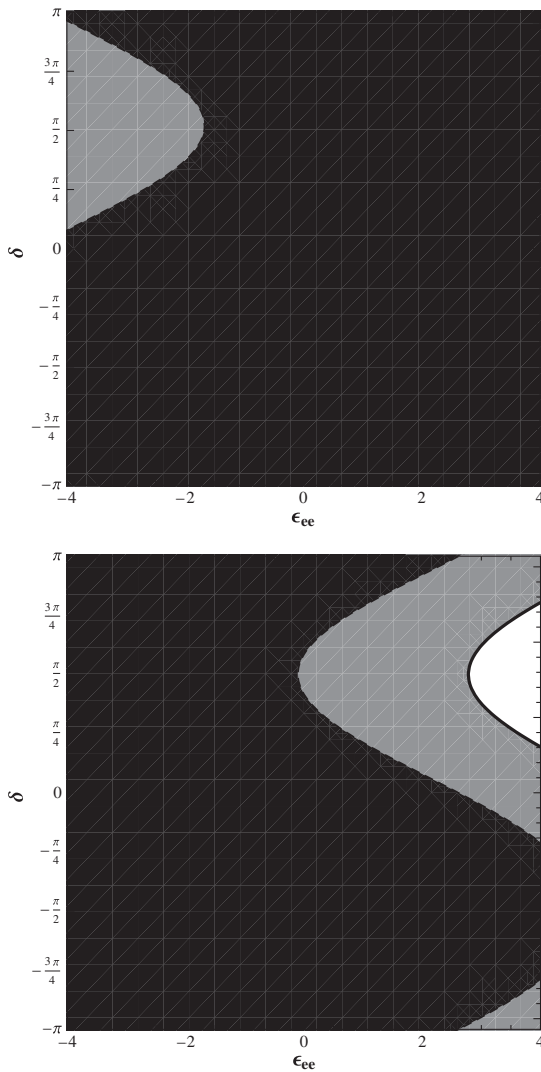


FIG. 1. Plot of $\epsilon_{ee} - \delta$ for real NSI in matter. Excluded region (white at 90% and grey + white region at 66% confidence level). Upper (lower) panel corresponds to normal (inverted) hierarchy.

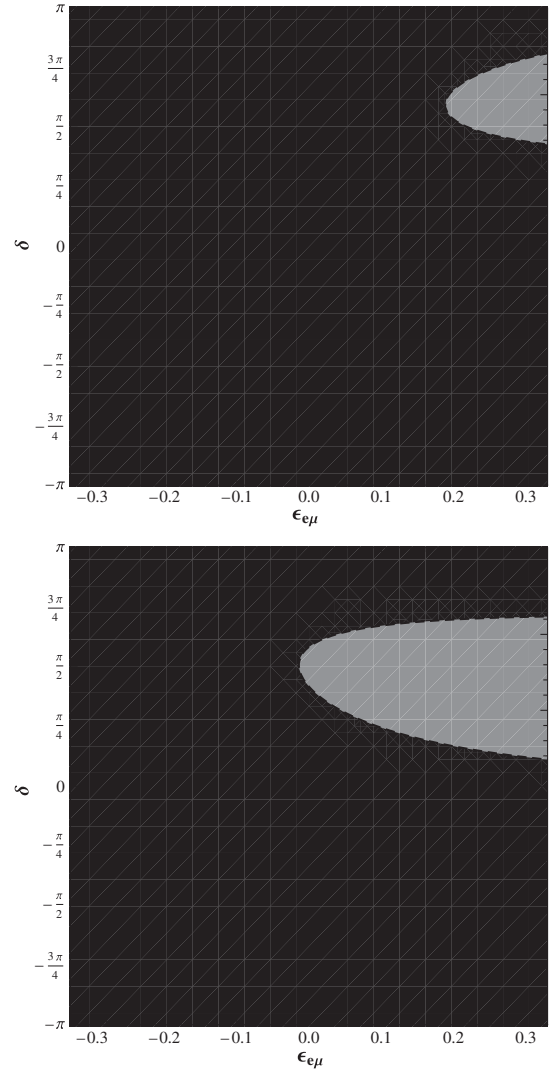


FIG. 2. Plot of $\epsilon_{e\mu} - \delta$ for real NSI in matter. Excluded region (white at 90% and grey + white region at 66% confidence level). Upper (lower) panel corresponds to normal (inverted) hierarchy.

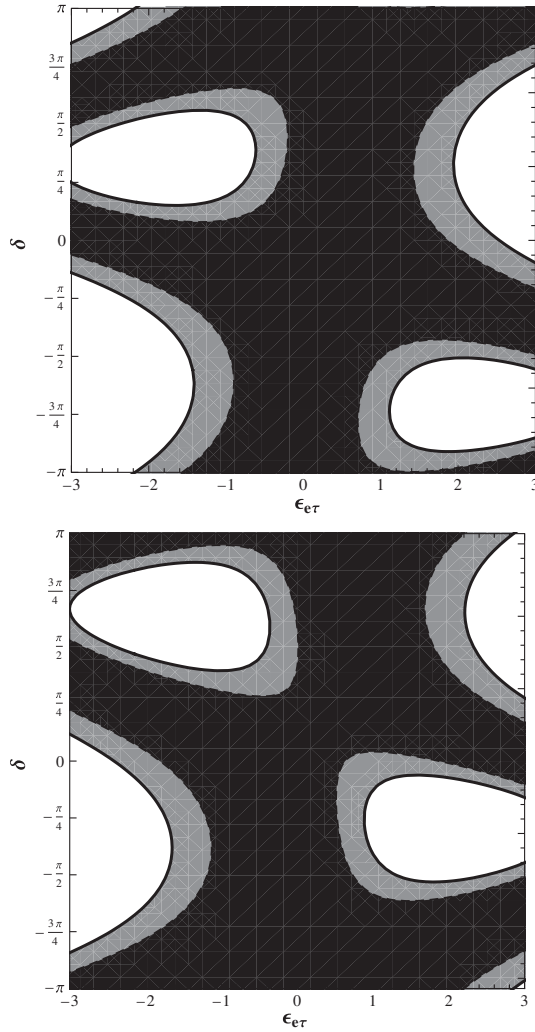


FIG. 3. Plot of $\epsilon_{e\tau} - \delta$ for real NSI in matter. Excluded region (white at 90% and grey + white region at 66% confidence level). Upper (lower) panel corresponds to normal (inverted) hierarchy.

positive values for both the hierarchies corresponding to T2K's 66% confidence level result only. In Fig. 3 $\epsilon_{e\tau}$ is significantly constrained. For normal hierarchy the negative (positive) value could be constrained up to about -0.2 (0.6) for certain values of δ corresponding to T2K's 66% confidence level result. For inverted hierarchy such constraints are even more stringent and for certain values of δ all negative values could be excluded. In Fig. 4 no constraint is obtained for $\epsilon_{\mu\mu}$ for normal hierarchy. However, for inverted hierarchy around $\delta = \pi/2$ all values are excluded corresponding to T2K's 66% confidence level result. In Fig. 5 for normal hierarchy no constraint is obtained on $\epsilon_{\mu\tau}$. For inverted hierarchy all negative values are excluded. In Fig. 6 there are stringent constraints on $\epsilon_{\tau\tau}$ particularly for positive values for normal hierarchy and negative values for inverted hierarchy corresponding to T2K's result at both 66 and 90% confidence level. A significant part of negative (positive) values of $\epsilon_{\tau\tau}$ are also excluded for normal (inverted) hierarchy corresponding to

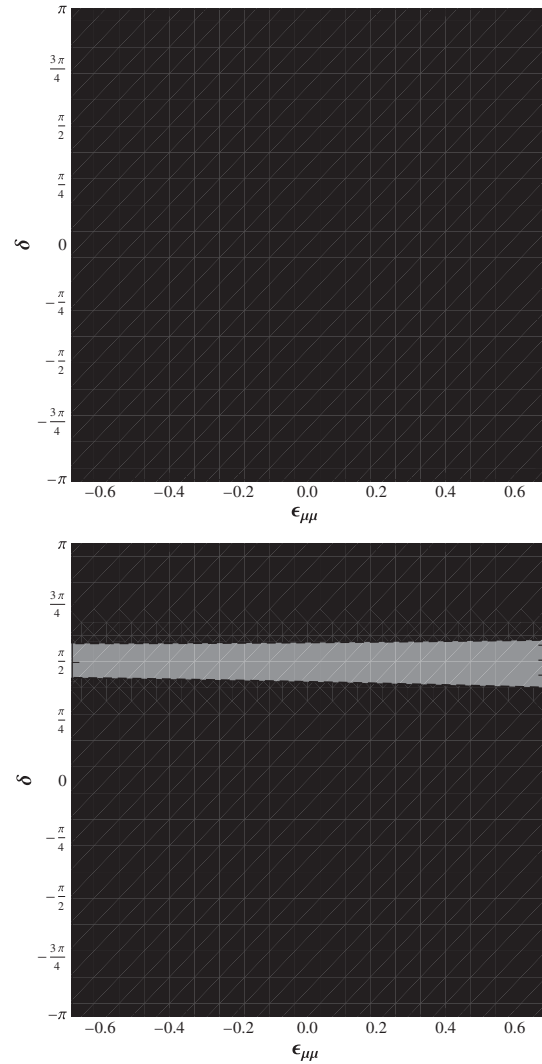


FIG. 4. Plot of $\epsilon_{\mu\mu} - \delta$ for real NSI in matter. Excluded region (white at 90% and grey + white region at 66% confidence level). Upper (lower) panel corresponds to normal (inverted) hierarchy.

the 66% confidence level. Interestingly, corresponding to T2K's 66% confidence level result one may obtain some constraints on $\epsilon_{\tau\tau}$ independent of δ from Fig. 6.

VII. CONCLUSION

In this work, using perturbation theory, we obtained the probability of oscillation $P_{\nu_\mu \rightarrow \nu_e}$ (suitable for a relatively short baseline of T2K and for large θ_{13} as evident from the Daya Bay experiment) up to order α^2 ($\alpha \equiv \frac{\Delta m_{21}^2}{\Delta m_{31}^2}$) by considering NSIs at the source and the detector as well as during propagation of neutrinos through matter. We have kept the standard matter interaction part in perturbed Hamiltonian that is appropriate for the baseline considered by T2K. In addition, we have considered two cases, namely, $\epsilon_{\alpha\beta}^m \sim \epsilon \sim 0.03$ and $\epsilon_{\alpha\beta}^m \sim \sqrt{\epsilon} \sim 0.18$ —the latter

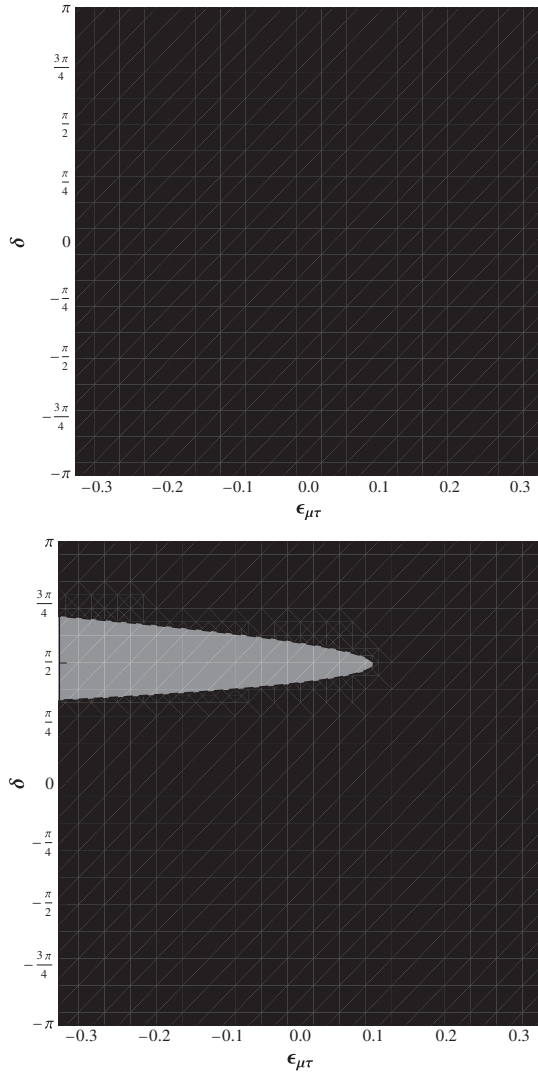


FIG. 5. Plot of $\epsilon_{\mu\tau} - \delta$ for real NSI in matter. Excluded region (white at 90% and grey + white region at 66% confidence level). Upper (lower) panel corresponds to normal (inverted) hierarchy.

corresponding to slightly larger NSI. In the expression of oscillation probability one can see that a flavor transition takes place at the source even before the propagation of neutrinos due to NSI at the source and the detector—which is the so-called zero distance effect. However, due to stringent constraints on these NSI parameters [5] we have assumed all of them of about 10^{-3} in our numerical analysis. Although there are good model-dependent bounds on NSI in matter (earthlike), these are not so strong if one likes to constrain them in a model-independent way [5]. In our numerical analysis, we have obtained constraints on various NSIs in matter in a model-independent way from neutrino oscillation experiments. Nevertheless, one may note as mentioned at the end of Sec. V that it is difficult to constrain very small NSIs in the relatively short baseline oscillation experiment like T2K. The recent Daya Bay result on mixing angle θ_{13} has helped us to give bounds on NSI depending on only one so far unknown

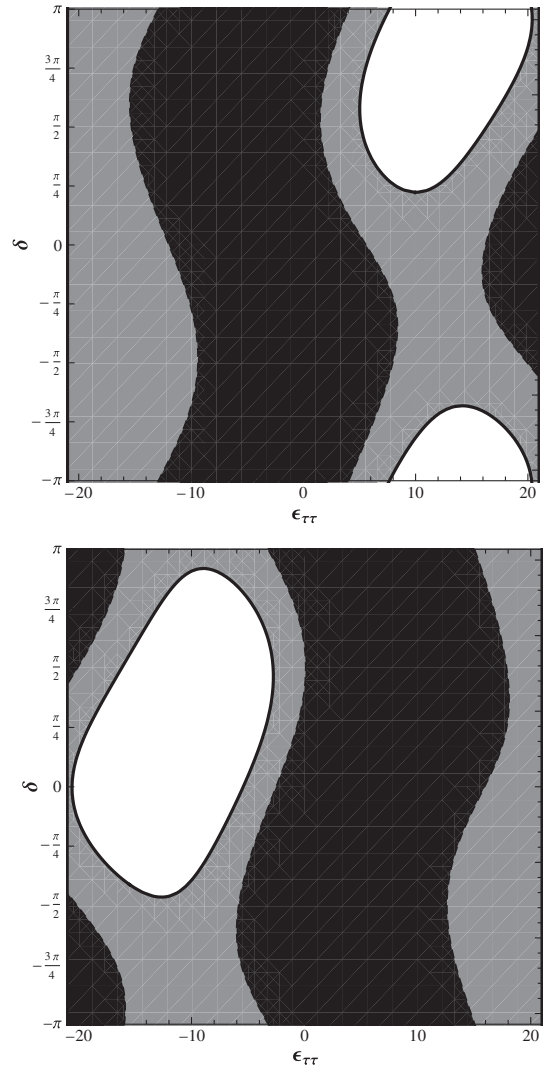


FIG. 6. Plot of $\epsilon_{\tau\tau} - \delta$ for real NSI in matter. Excluded region (white at 90% and grey + white region at 66% confidence level). Upper (lower) panel corresponds to normal (inverted) hierarchy.

parameter δ in neutrino mixing matrix. Once one knows this phase from some short baseline neutrino oscillation experiments, one may expect the better understanding about the possible strength of NSI. Depending on the δ value, a significant constraint on $\epsilon_{e\tau}^m$ and $\epsilon_{\tau\tau}^m$ could be possible for both normal and inverted neutrino mass hierarchies. One may note here that in Sec. IV $\epsilon_{\tau\tau}^m$ has not appeared in the expression of oscillation probability, but still we have obtained a significant constraint on it because of its very high presently allowed model-independent values [5]. Our studies indicate that while finding neutrino oscillation parameters it might be important to search for any possible evidence of NSIs even in the relatively shorter baseline neutrino oscillation experiments although longer ones are in general preferred. In the coming years the precision measurement of neutrino oscillation parameters and the NSI parameters in neutrino oscillation experiments

could be challenging and could even show the evidence of NSIs.

ACKNOWLEDGMENTS

Two of us (R. A. and A. D.) acknowledge the hospitality of the Indian Association for Cultivation of Science, Kolkata where this work was initiated. S. C. and A. D. thank the Council of Scientific and Industrial Research, Government of India. S. C. would also like to thank Kush

Saha, Pradipta Ghosh, and Subhadeep Mondal for helpful discussions and Tommy Ohlsson for his thoughtful insights that helped us greatly. S. R. acknowledges the kind hospitality provided by the Helsinki Institute of Physics and the University of Helsinki, Finland and CERN theory division while this work was in progress. R. A. and S. R. would like to acknowledge the hospitality provided by the organizers of WHEPP-XII held at Mahabaleshwar, India, where this work was completed.

-
- [1] K. Abe *et al.* (T2K Collaboration), *Phys. Rev. Lett.* **107**, 041801 (2011).
- [2] F. P. An *et al.* (DAYA-BAY Collaboration), *Phys. Rev. Lett.* **108**, 171803 (2012).
- [3] J. K. Ahn *et al.* (RENO Collaboration), *Phys. Rev. Lett.* **108**, 191802 (2012).
- [4] D. Meloni, T. Ohlsson, and H. Zhang, *J. High Energy Phys.* **04** (2009) 033.
- [5] C. Biggio, M. Blennow, and E. Fernández-Martínez, *J. High Energy Phys.* **08** (2009) 090.
- [6] Y. Grossman, *Phys. Lett. B* **359**, 141 (1995).
- [7] T. Ota, J. Sato, and N. a. Yamashita, *Phys. Rev. D* **65**, 093015 (2002).
- [8] P. Huber, T. Schwetz, and J. W. F. Valle, *Phys. Rev. D* **66**, 013006 (2002).
- [9] T. Ota and J. Sato, *Phys. Lett. B* **545**, 367 (2002).
- [10] M. C. Gonzalez-Garcia, Y. Grossman, A. Gusso, and Y. Nir, *Phys. Rev. D* **64**, 096006 (2001).
- [11] A. M. Gago, M. M. Guzzo, H. Nunokawa, W. J. C. Teves, and R. Zukanovich Funchal, *Phys. Rev. D* **64**, 073003 (2001).
- [12] P. Huber and J. W. F. Valle, *Phys. Lett. B* **523**, 151 (2001).
- [13] P. Huber, T. Schwetz, and J. W. F. Valle, *Phys. Rev. Lett.* **88**, 101804 (2002).
- [14] M. Campanelli and A. Romanino, *Phys. Rev. D* **66**, 113001 (2002).
- [15] S. Davidson, C. Pena-Garay, N. Rius, and A. Santamaria, *J. High Energy Phys.* **03** (2003) 011.
- [16] M. Honda, N. Okamura, and T. Takeuchi, [arXiv:hep-ph/0603268](https://arxiv.org/abs/hep-ph/0603268).
- [17] N. Kitazawa, H. Sugiyama, and O. Yasuda, [arXiv:hep-ph/0606013](https://arxiv.org/abs/hep-ph/0606013).
- [18] M. Blennow, T. Ohlsson, and J. Skrotzki, *Phys. Lett. B* **660**, 522 (2008).
- [19] S. Bergmann, M. M. Guzzo, P. C. de Holanda, P. I. Krastev, and H. Nunokawa, *Phys. Rev. D* **62**, 073001 (2000).
- [20] Z. Berezhiani, R. S. Raghavan, and A. Rossi, *Nucl. Phys. B* **638**, 62 (2002).
- [21] A. Friedland, C. Lunardini, and C. Pena-Garay, *Phys. Lett. B* **594**, 347 (2004).
- [22] O. G. Miranda, M. A. Tortola, and J. W. F. Valle, *J. High Energy Phys.* **10** (2006) 008.
- [23] M. C. Gonzalez-Garcia, M. M. Guzzo, P. I. Krastev, H. Nunokawa, O. L. G. Peres, V. Pleitez, J. W. F. Valle, and R. Zukanovich Funchal, *Phys. Rev. Lett.* **82**, 3202 (1999).
- [24] S. Bergmann, Y. Grossman, and D. M. Pierce, *Phys. Rev. D* **61**, 053005 (2000).
- [25] N. Fornengo, M. Maltoni, R. Tomas, and J. W. F. Valle, *Phys. Rev. D* **65**, 013010 (2001).
- [26] M. C. Gonzalez-Garcia and M. Maltoni, *Phys. Rev. D* **70**, 033010 (2004).
- [27] A. Friedland, C. Lunardini, and M. Maltoni, *Phys. Rev. D* **70**, 111301 (2004).
- [28] S. Bergmann and Y. Grossman, *Phys. Rev. D* **59**, 093005 (1999).
- [29] M. Honda, N. Okamura, and T. Takeuchi, [arXiv:hep-ph/0603268](https://arxiv.org/abs/hep-ph/0603268).
- [30] A. Friedland and C. Lunardini, *Phys. Rev. D* **74**, 033012 (2006).
- [31] A. Bueno, M. Campanelli, M. Laveder, J. Rico, and A. Rubbia, *J. High Energy Phys.* **06** (2001) 032.
- [32] J. Kopp, M. Lindner, and T. Ota, *Phys. Rev. D* **76**, 013001 (2007).
- [33] J. Kopp, T. Ota, and W. Winter, *Phys. Rev. D* **78**, 053007 (2008).
- [34] R. Adhikari, S. K. Agarwalla, and A. Raychaudhuri, *Phys. Lett. B* **642**, 111 (2006).
- [35] G. L. Fogli, E. Lisi, A. Mirizzi, and D. Montanino, *Phys. Rev. D* **66**, 013009 (2002).
- [36] H. Duan, G. M. Fuller, J. Carlson, and Y. Z. Qian, *Phys. Rev. Lett.* **97**, 241101 (2006).
- [37] A. Esteban-Pretel, R. Tomas, and J. W. F. Valle, *Phys. Rev. D* **76**, 053001 (2007).
- [38] G. Mangano, G. Miele, S. Pastor, T. Pinto, O. Pisanti, and P. D. Serpico, *Nucl. Phys. B* **756**, 100 (2006).
- [39] K. M. Belotsky, A. L. Sudarikov, and M. Y. Khlopov, *Yad. Fiz.* **64**, 1718 (2001) [*Phys. At. Nucl.* **64**, 1637 (2001)].
- [40] J. S. Diaz, [arXiv:1109.4620](https://arxiv.org/abs/1109.4620); V. A. Kostelecky and M. Mewes, *Phys. Rev. D* **69**, 016005 (2004).
- [41] A. Friedland, M. L. Graesser, I. M. Shoemaker, and L. Vecchi, [arXiv:1111.5331](https://arxiv.org/abs/1111.5331).
- [42] A. Palazzo and J. W. F. Valle, *Phys. Rev. D* **80**, 091301 (2009); A. Palazzo, *Phys. Rev. D* **83**, 101701 (2011).
- [43] T. Ohlsson and H. Zhang, *Phys. Lett. B* **671**, 99 (2009).
- [44] T. Kikuchi, H. Minakata, and S. Uchinami, *J. High Energy Phys.* **03** (2009) 114.
- [45] H. Minakata, *Acta Phys. Pol. B* **40**, 3023 (2009).
- [46] K. Asano and H. Minakata, *J. High Energy Phys.* **06** (2011) 022.

- [47] E. Fernandez-Martinez, M. B. Gavela, J. Lopez-Pavon, and O. Yasuda, *Phys. Lett. B* **649**, 427 (2007).
- [48] S. Antusch, C. Biggio, E. Fernández-Mártínez, M. B. Gavela, and J. López-Pavón, *J. High Energy Phys.* **10** (2006) 084.
- [49] P. Langacker and D. London, *Phys. Rev. D* **38**, 907 (1988).
- [50] W. Rodejohann, *Phys. Lett. B* **684**, 40 (2010).
- [51] J. Kopp, M. Lindner, T. Ota, and J. Sato, *Phys. Rev. D* **77**, 013007 (2008).
- [52] B. Pontecorvo, *Zh. Eksp. Teor. Fiz.* **34**, 247 (1957) [*Sov. Phys. JETP* **7**, 172 (1958)].
- [53] Z. Maki, M. Nakagawa, and S. Sakata, *Prog. Theor. Phys.* **28**, 870 (1962).
- [54] E. K. Akhmedov, R. Johansson, M. Lindner, T. Ohlsson, and T. Schwetz, *J. High Energy Phys.* **04** (2004) 078.
- [55] M. Freund, *Phys. Rev. D* **64**, 053003 (2001).
- [56] B. Kayser, in *Proceedings of the 32nd SLAC Summer Institute on Particle Physics (SSI 2004): Nature's Greatest Puzzles, Menlo Park, California, 2004*, eConf C040802, L004 (2004).
- [57] L. Wolfenstein, *Phys. Rev. D* **17**, 2369 (1978).
- [58] S. P. Mikheyev and A. Y. Smirnov, *Prog. Part. Nucl. Phys.* **23**, 41 (1989).
- [59] J. Kopp, Ph.D. thesis, Ruprecht-Karls-Universitt Heidelberg, 2009.
- [60] S. Toshev, *Mod. Phys. Lett. A* **06**, 455 (1991).
- [61] S. Goswami and T. Ota, *Phys. Rev. D* **78**, 033012 (2008).
- [62] Z. z. Xing and S. Zhou, *Phys. Lett. B* **666**, 166 (2008).
- [63] S. Luo, *Phys. Rev. D* **78**, 016006 (2008).
- [64] G. Altarelli and D. Meloni, *Nucl. Phys.* **B809**, 158 (2009).
- [65] A. Cervera, A. Donini, M. B. Gavela, J. J. Gomez Cadenas, P. Hernandez, O. Mena, and S. Rigolin, *Nucl. Phys.* **B579**, 17 (2000); **B593**, 731(E) (2001).
- [66] A. Friedland, C. Lunardini, and C. Pena-Garay, *Phys. Lett. B* **594**, 347 (2004).
- [67] A. Friedland and C. Lunardini, *Phys. Rev. D* **72**, 053009 (2005).